BIOCHEMISTRY
including biophysical chemistry & molecular biology

Article

pubs.acs.org/biochemistry

# Terminal Residue Hydrophobicity Modulates Transmembrane Helix–Helix Interactions

Derek P. Ng and Charles M. Deber*

Division of Molecular Structure & Function, Research Institute, Hospital for Sick Children, Toronto, Ontario M5G 0A4, Canada
Department of Biochemistry, University of Toronto, Toronto, Ontario M5S 1A8, Canada

Supporting Information

**ABSTRACT:** Central to the formation of tertiary structure in membrane protein folding is the presence of amino acid sequence motifs (such as "small-XXX-small" segments) in the TM segments that promote interaction-compatible surfaces through which the TM $\alpha$-helices interact. Here, we sought to elucidate additional factors that may work in tandem to dictate the ultimate interaction fate of TM-embedded segments. In this context, we used proteolipid protein (PLP), the major protein from central nervous system myelin for which mutant-dependent non-native oligomerization has been implicated in neurological disorders, to explore the specific effects of TM boundary residues (the membrane entry and exit points), keying on the secondary structure and self-association of peptides corresponding to the PLP TM2 $\alpha$-helix (wild-type sequence $^{66}$AFQYVIYGTASFFFLYGALLLAEGF$^{90}$). Using gel electrophoresis, circular dichroism, and Förster resonance energy transfer in the membrane-mimetic detergent sodium dodecyl sulfate (SDS), we found that mutation of F90 to residues such as A, I, L, or V maintains the onset of TM2–TM2 dimerization, whereas mutation to E, G, Q, N, S, or T abrogates dimer formation. We attribute this sensitivity to changes in local hydrophobicity, viz., a decrease in hydrophobicity reduces local lipid–peptide interactions, which in turn disrupts peptide $\alpha$-helicity and hence the effectiveness of an incipient interaction-compatible surface. Our results show that the secondary structure and oligomeric state of PLP TM2 Lys-tagged peptides are significantly modulated by the specific nature of their C-terminal boundary residue, thus providing insight as to how point mutations, particularly where they produce disease states, can compromise the folding process.

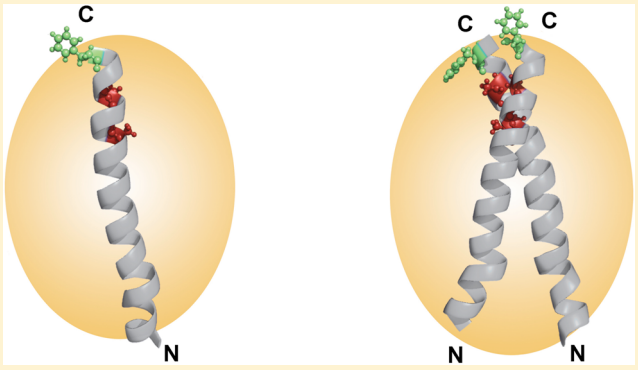


The fundamental process by which an $\alpha$-helical membrane protein attains its ultimate structure has been depicted as two energetically distinct stages where the TM segments are first threaded into the membrane bilayer as stable $\alpha$-helices and where they then laterally interact to form the correct tertiary and/or quaternary structures.[1] Central to the second stage of this model is the presence of amino acid sequence motifs in the TM segments that provide interaction-compatible surfaces through which the TM $\alpha$-helices assemble.[1] Yet, a growing number of examples indicate that the presence of sequence motifs is likely a necessary, but not always a sufficient, condition for directing helix–helix interactions and that a multitude of factors work together to dictate the interaction fate of TM-embedded segments,[2] including the folding of extramembranous loops and domains,[3] lipid–protein interactions,[4] bilayer bulk properties,[5,6] and the presence of small molecules and other membrane proteins.[4,7] In addition, the two stages of the model are not necessarily independent of one another; for example, the specific interactions of TM helices in the human adenosine $A_{2A}$ receptor can increase and stabilize the $\alpha$-helicity of the segments themselves.[8]

This diverse repertoire of factors likely provides the biological opportunity to fine-tune and/or regulate membrane protein folding, structure, and function from multiple control points. For example, the change in bilayer thickness of the membranes that constitute the secretory pathway, combined with the effect of hydrophobic mismatch on TM helix interactions, may provide a mechanism for inhibiting membrane protein functionality until the protein has been delivered to its final membrane destination.[4] The same argument could be used to explain why some TM signaling proteins have enhanced activities in cholesterol-rich lipid domains (because the presence of cholesterol may increase bilayer thickness as well as change lipid acyl chain order).[4,9,10] In the case of myelin proteolipid protein (PLP), hydrophobic mismatch between the TM helices and the ER and plasma membranes may play a role in the delayed oligomerization of wild-type PLP.[11,12] Bilayer thickness is known to differ between the ER and plasma membranes.[13,14] In the ER, the thinner

**Received:** March 13, 2014
**Revised:** May 23, 2014
**Published:** May 23, 2014

   dx.doi.org/10.1021/bi500317h | *Biochemistry* 2014, 53, 3747–3757

membrane may decrease TM helicities and result in a destabilization of the PLP oligomer. However, when the protein is finally delivered to the plasma membrane, the increase in bilayer thickness may increase TM helicities, allowing PLP to oligomerize.

In this context, one aspect of TM helices that has received relatively little attention relates to their boundaries, viz., where does the TM helix enter and exit the membrane? These boundaries have been traditionally challenging to establish experimentally, as demonstrated by the fact that TM prediction programs widely differ in this aspect of prediction.[15] Previously, we explored the effects of TM $\alpha$-helix boundary residues on the properties of a TM peptide comprising the TM2 $\alpha$-helix of PLP (residues 66−89), finding that both its secondary structure and oligomerization potential were drastically altered by the inclusion or deletion of a single residue at the peptide C-terminus.[16] We hypothesized that this shift in peptide properties was due to a change in the local TM hydrophobicity at the peptide C-terminus, ostensibly at the water/membrane interface, and explored the implications of this observation vis-à-vis a discrete role for TM boundary residues as a directing factor in membrane protein folding. In the current study, we further examine and codify this hypothesis by expanding our initial set of PLP TM2 peptides, and we perform biophysical analysis of their residue-dependent conformational and oligomeric properties. Our findings that TM2−TM2 association is directly dependent on a single change in the segment C-terminal residue emphasize the importance of helix stabilizing/destabilizing boundary residues in TM segments and, as such, may play an important role in the folding of membrane proteins *in vivo*.

## EXPERIMENTAL PROCEDURES

**Peptide Synthesis and Labeling.** Peptides were synthesized using solid-phase Fmoc chemistry[17] on a PS3 peptide synthesizer (Protein Technologies, Inc.) using the protocol from the manufacturer. A 4-fold excess of amino acids on a 0.1 mmol scale was used with the HATU/DIEA activator pair. An amidated C-terminus was produced using a low-load (0.18−0.22 mmol/g) PAL−PEG−PS resin. For FRET experiments, peptides were labeled with dansyl chloride and dabsyl chloride (Molecular Probes) as follows: 100 mg of resin containing covalently attached peptide (such that the only reactive site is the amino group of the N-terminal residue) was incubated overnight in 10 mg of label with 1 mL of DMF and 50 $\mu$L of DIEA (room temperature, in the dark, under nitrogen, with stirring). This reaction was repeated to enhance labeling. Peptides were cleaved from the resin using a cocktail consisting of 88% TFA, 5% phenol, 5% ultrapure water, and 2% TIPS. The cleaved peptides were subsequently precipitated and washed with ice-cold diethyl ether, air-dried, and redissolved in ultrapure water. For purification, peptides were loaded onto a C4 preparative RP-HPLC column (Phenomenex), and the major peaks from water/2-propanol or water/acetonitrile gradients were collected. Peptide MWs and purity were confirmed by MALDI mass spectrometry. The labeling efficiencies of dansyl- and dabsyl-labeled peptides were greater than 90 and 95%, respectively (as estimated from mass spectrometry). Samples were lyophilized, redissolved in ultrapure water, and stored at −20 °C.

**Peptide Quantitation.** Peptide concentrations were estimated using the adapted methodology from Rath et al.[18] and summarized as follows. The absorbance levels at 470.0 nm of serial dilutions of TFE-solubilized dabsyl-peptides were used to calculate the peptide concentration in the dilutions (via molar extinction coefficient of dabsyl-glycine in TFE at 470.0 nm of $2.96 \times 10^4$ cm$^{-1}$ M$^{-1}$). Circular dichroism (CD) spectra of the quantitated dabsyl-peptide solutions in TFE were subsequently obtained in a 0.1 cm path length cuvette, and plots of ellipticity at 222 nm per residue per centimeter of path length versus dabsyl-peptide concentration in TFE were constructed. The slope of the best-fit line of each plot was used to determine ellipticity coefficients of each dabsyl-peptide. These ellipticity coefficients were used to quantitate solutions of unlabeled- and dansyl-peptide solutions in TFE from their CD spectra, and the original concentrations of the peptide stocks in water were back-calculated.

**Buffers.** The buffer used consisted of 10 mM borate, 10 mM phosphate, and 10 mM acetate at pH 7.3. The peptide-to-SDS ratio was kept constant at 1:7000 (i.e., 70 mM and 105 mM SDS were used for FRET and CD, respectively).

**Circular Dichroism (CD) Spectroscopy.** Peptide samples were prepared at 15 $\mu$M. Samples in aqueous buffer or aqueous buffer with detergent were allowed to equilibrate overnight at room temperature prior to being read in a Jasco J-720 circular dichroism spectropolarimeter. TFE samples were read within 30 min of preparation. The path length of the cuvette was 0.1 cm. Spectral scans were performed from 250 to 190 nm, with a step resolution of 0.1 nm, a bandwidth of 2 nm, and a speed of 50 nm/min. Three scans were acquired and averaged per sample, and all experiments were performed in triplicate. Background spectra without peptide were subtracted.

Percent helicities were calculated on the basis of the following formulas

$$\text{percent helicity} = \frac{\text{MRE}_{222\text{nm}}}{\text{MRE}_{222\text{nm,max}}} \times 100$$

$$\text{MRE}_{222\text{nm,max}} = \frac{[(n - 4.6)(-40\,000)]}{n}$$

where $\text{MRE}_{222\text{nm}}$ is the peptide molar residue ellipticity (MRE) at 222 nm, $\text{MRE}_{222\text{nm,max}}$ is the theoretical maximum MRE of the peptide (i.e., the MRE expected for a peptide in a 100% helical conformation), and $n$ is the number of residues in the peptide.[19,20] The $\text{MRE}_{222\text{nm,max}}$ of a 33-residue peptide is calculated to be −34 424 degree cm$^2$ dmol$^{-1}$.

**SDS-PAGE.** Gel boxes, gels (18% Tris-glycine), and buffers were purchased from Novex Corp. PAGE was conducted according to the manufacturer's instructions. Peptides were resuspended in sample buffer and incubated at room temperature for >15 min prior to being loaded on the gel. Peptides were visualized with Sypro Ruby protein gel stain (Invitrogen) following the manufacturer's instructions. Apparent molecular weights ($\text{MW}_{\text{app}}$) were estimated from the migration of Novex Sharp unstained protein standards (Invitrogen) and were averaged from at least three independent gel runs. Decreases in the rate of migration from the lysine tags were taken into account when calculating the $\text{MW}_{\text{app}}$;[21] ImageJ (National Institutes of Health) was used to analyze the gels.

**Fluorescence Resonance Energy Transfer (FRET) Titrations.** FRET experiments were conducted using dansyl-labeled peptides (donor) in the presence of increasing mole fractions of dabsyl-labeled peptides (acceptor). The dansyl-labeled peptide concentration was maintained at 2 $\mu$M as the mole fraction of dabsyl-labeled peptide was increased for a total peptide concentration of 10 $\mu$M. The addition of unlabeled

**Table 1. Sequences of the PLP TM2 Peptides Containing Phe-90 Substitutions**

| peptide | sequence[a] | MW (Da) |
|---|---|---|
| TM2-F (WT) | KKKK-$^{66}$AFQYVIYGTASFFFLYGALLLAEG**F**$^{90}$-KKKK | 3834 |
| TM2-A | KKKK-AFQYVIYGTASFFFLYGALLLAEG**A**-KKKK | 3759 |
| TM2-E | KKKK-AFQYVIYGTASFFFLYGALLLAEG**E**-KKKK | 3816 |
| TM2-G | KKKK-AFQYVIYGTASFFFLYGALLLAEG**G**-KKKK | 3745 |
| TM2-H | KKKK-AFQYVIYGTASFFFLYGALLLAEG**H**-KKKK | 3825 |
| TM2-I | KKKK-AFQYVIYGTASFFFLYGALLLAEG**I**-KKKK | 3800 |
| TM2-L | KKKK-AFQYVIYGTASFFFLYGALLLAEG**L**-KKKK | 3800 |
| TM2-N | KKKK-AFQYVIYGTASFFFLYGALLLAEG**N**-KKKK | 3801 |
| TM2-Q | KKKK-AFQYVIYGTASFFFLYGALLLAEG**Q**-KKKK | 3816 |
| TM2-S | KKKK-AFQYVIYGTASFFFLYGALLLAEG**S**-KKKK | 3774 |
| TM2-T | KKKK-AFQYVIYGTASFFFLYGALLLAEG**T**-KKKK | 3788 |
| TM2-V | KKKK-AFQYVIYGTASFFFLYGALLLAEG**V**-KKKK | 3787 |

[a]Mutated residues are underlined.

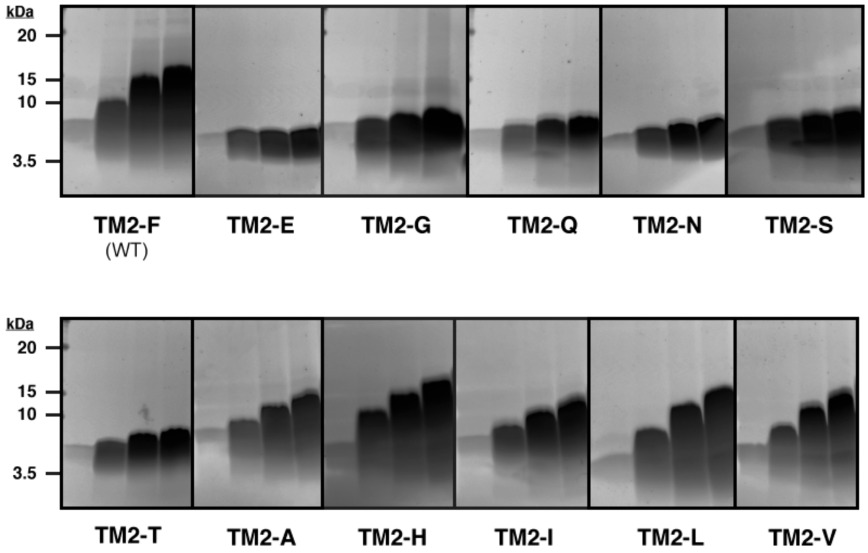


**Figure 1.** Effect of Phe-90 mutations on SDS-PAGE migration. TM2 peptides containing the Phe-90 mutations were loaded onto 18% Tris-glycine gels at increasing amounts of peptide: 0.05, 1.0, 2.5, and 3.5 $\mu$g (increasing from left to right per gel). The gels were stained and visualized using Sypro Ruby protein stain.

peptide was used to keep the total peptide concentration constant. Peptides were mixed prior to the addition of the buffer and SDS. Samples were then allowed to equilibrate at room temperature overnight before being read in either a 0.1 cm cuvette by a Photon Technology International C-60 spectrofluorimeter or a 96-well fluorescence plate by a Molecular Devices SpectraMax Gemini EM microplate spectrofluorometer. The excitation wavelength was set to 341 nm with a 4 nm bandpass, and emission spectra were recorded from 450 to 600 nm with a 4 nm bandpass at a scanning speed of 1 nm/0.3 s and an average of three scans. All samples were analyzed in triplicate. Spectra were integrated between 450 and 600 nm using the software provided by the manufacturer. Integrated total fluorescence intensities at each point in the titration ($F$) were normalized by the initial integrated total fluorescence intensity in the absence of acceptor peptide ($F_0$). The mole fraction acceptor ($P_A$) was calculated according to the relation

$$P_A = \frac{[\text{acceptor peptide}]}{[\text{total peptide}]}$$

Fitting the data to the following equation allows us to estimate the oligomeric state of the peptide[22]

$$\frac{F}{F_0} = (1 - k) + k(1 - P_A)^{n-1}$$

where $F/F_0$ is the ratio of the donor fluorescence intensity in the presence of acceptor and the donor fluorescence intensity in the absence of the acceptor, $P_A$ is the ratio of acceptor, $n$ is the number of peptides in the oligomer, and $k = (f_D - f_Q)/f_D$, where $f_D$ and $f_Q$ are the molar fluorescence of donor and quenched donor, respectively.

For a monomer−dimer equilibrium (i.e., $n = 2$), the above equation simplifies into a linear relationship

$$\frac{F}{F_0} = 1 - kP_A$$

If the distance between the donor and acceptor FRET pair is less than the Förster radius, the slope ($k$) can be used as an estimate of the strength of helix−helix interactions (i.e., the fraction of peptides in the dimeric state).[23]

For FRET competition experiments, a 5 $\mu$M dansyl-labeled peptide solution was mixed with either 5 $\mu$M unlabeled peptide,


dx.doi.org/10.1021/bi500317h | *Biochemistry* 2014, 53, 3747−3757

5 $\mu$M dabsyl-labeled peptide, or 5 $\mu$M dabsyl and 20 $\mu$M unlabeled peptide.

## RESULTS

**SDS-PAGE Analysis of PLP TM2 Peptides with a Varying C-terminal Residue.** To investigate the sensitivity of TM structure to the choice, and/or the presence or absence, of amino acids at the C-terminus,[16] we synthesized a library of PLP TM2 peptides where the wild-type C-terminal Phe-90 residue was mutated individually to a diverse range of amino acids (nonpolar, polar, and charged) (Table 1). Cys and Pro were avoided because of their unique properties (i.e., disulfide forming potential and inability to form a backbone H-bond, respectively). Trp and Tyr were not selected because they have been previously shown to have preferences for membrane-interface regions of bilayers.[24,25] For Asp, Lys, and Arg, Glu adequately represents the charged nature of these amino acids. Similarly, Met was not chosen, because Leu and Ile adequately represent its nonpolarity. The peptide termini were previously determined by obtaining the consensus sequence output of several TM predicting algorithms.[16] The sequence lengths of the new peptides were kept constant relative to TM2-F in order to elucidate against a common background any additional factors (besides length itself) that may be modulating the properties of a given mutant peptide. A total of eight Lys residues were "tagged" to the ends of the peptide (four Lys residues on each terminus) to increase solubility while preserving the native properties of the hydrophobic TM segment.

In order to examine their oligomerization potential, SDS-PAGE gels were run where the total amount of each peptide loaded was titrated as a function of increasing peptide concentration (Figure 1). In a consideration of the factors relating to interpretation of these gels, it should first be noted that the peptides (as monomers) with hydrophobic C-terminal residues will migrate with higher apparent MWs (vs the soluble protein standards) than those with more hydrophilic residues because of the greater attraction and binding of SDS molecules;[26] this effect is manifested, for example, by noting the apparent MW of the peptide band at the lowest concentration point (left lane) on the TM2-F gel (~6.5 kDa) versus that of the TM2-E gel (~5.3 kDa). The difference in apparent MWs (~1.2 kDa) is significantly greater than the difference in formula weights (~0.02 kDa) of these two peptides. That said, the further slowing of peptide migration rates could then be attributed to an (average) increase in peptide oligomeric state(s).

The SDS-PAGE titration profiles showed differences among the peptides. In general, the behavior of the peptides could be divided into (1) the group with migration rates that slowed and (2) the group with migration rates that showed little or no change as a function of increasing peptide concentrations. To further quantitate these results, the $MW_{app}$ of the bands was normalized to the $MW_{app}$ of the 0.05 $\mu$g band for each peptide in order to remove any effects resulting from differential SDS-binding.[26] The differences in titration profiles among the peptides were statistically significant (two-way ANOVA, $p$ value < 0.001 for the interaction between peptide loading amounts and mutants). The peptides with Phe-90 mutated to Ala, His, Ile, Leu, and Val showed titration profiles similar to that of the WT Phe-90 peptide (see Supporting Information Figure S1); for each of these peptides, the normalized $MW_{app}$'s of the bands showed statistically significant increases as the peptide loading amount was increased (Dunnett multiple comparison test, $p$ values < 0.001). In contrast, mutations at position 90 to Glu, Gly, Gln, Asn, Ser, and Thr changed the titration behavior of the peptides compared to that of the WT: this latter group of peptides showed no statistically significant change in the normalized $MW_{app}$ as a function of peptide loading amount. These results immediately established that the nature of the amino acid at the C-terminus of the TM2 peptide has a significant impact on the peptide's ability to self-associate.

SDS-FRET dabsyl titration experiments were then performed to quantitate the oligomerization level of position 90 mutations (Figure 2A). In general, as the acceptor mole fraction for the peptide was increased, we found that the fluorescence signal decreased, and this trend did not deviate significantly from linearity (based on runs test). Slopes were significantly greater than zero (extra sum-of-squares F test, $p$ < 0.0001), indicating that the peptides are largely dimeric. However, the slopes differed among the mutants (extra sum-of-squares F test, $p$ < 0.0001). Given that the distance between a FRET pair is smaller than the Förster radius, the slope of the titration can be interpreted as the fraction of molecules in the dimeric state

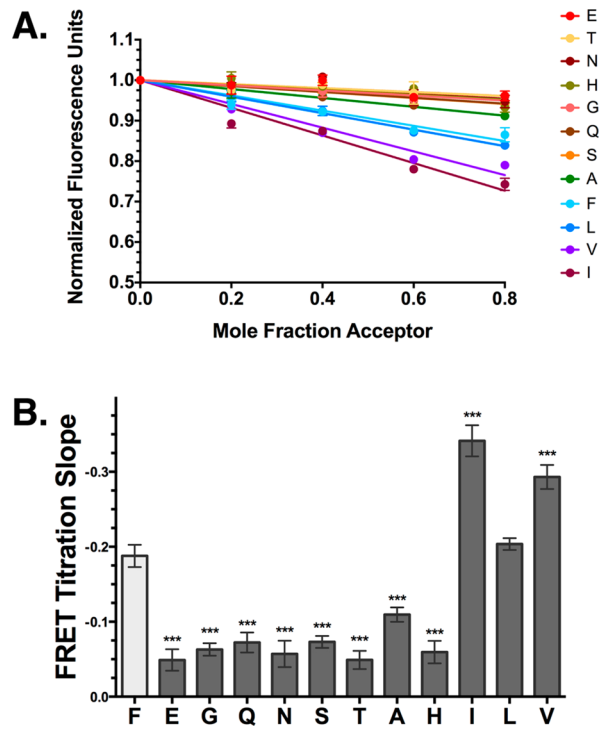


**Figure 2.** SDS-FRET dabsyl titration analysis of the Phe-90 mutated TM2-F peptides. (A) SDS-FRET titration. Dansyl-labeled peptides (donor) were titrated with an increasing mole fraction of dabsyl-labeled peptides (acceptor) in 70 mM SDS, 10 mM borate, 10 mM phosphate, and 10 mM acetate (pH 7.3). The total peptide concentration was kept constant at 10 $\mu$M by the addition of unlabeled peptide. Dansyl-labeled donor peptides were excited at 341 nm, and emission was measured from 450 to 650 nm. Plots were generated and data were fit as described in the Experimental Procedures; the lines shown represent the best fit to each data set. Error bars correspond to the standard deviation of at least three experiments. (B) FRET slope analysis. The slopes from the linear fit of the FRET titration data were extracted and plotted. Error bars correspond to the standard error of the mean. The mutant peptides were compared to WT TM2-F using the Dunnet multiple comparison test. ***, $p$ < 0.001.

($f_D$) and/or percent dimer.[27] Because the average $C_\alpha$–$C_\alpha$ distance between two TM $\alpha$-helices in membrane proteins is 6.0 ± 1.1 Å[28] and the Förster radius for our FRET pair is 33 Å, we used the slopes derived from linear fits of our data as estimates of the fraction dimer in each peptide (Figure 2B). Similar to the SDS-PAGE results, the FRET experiments indicate that the amino acid identity at position 90 of the sequence can affect the helix–helix interactions of the peptide. Mutations of Phe-90 to Glu, Gly, Gln, Asn, Ser, Thr, Ala, and His are destabilizing (Dunnet multiple comparison test, $p < 0.001$), whereas mutations to Ile and Val increase helix–helix interactions ($p < 0.001$). Mutation to Leu showed no significant effect on the ability of the peptide to dimerize.

In these experiments, the FRET titration slope (fraction dimer) of the WT (and mutants) did not reach −1.0. In fact, the peptide that had the greatest slope was TM2-I, at −0.34 ± 0.02. The low proportion of dimer is likely due to the total peptide concentration used in the experiment (10 $\mu$M). As seen in SDS-PAGE, the shift in oligomeric state is a function of peptide amount. In a similar manner, increasing the total peptide concentration in the FRET experiment will likely shift the proportion of peptide toward the dimeric state. Figure S3 (Supporting Information) shows a graph of the SDS-FRET titration slopes versus SDS-PAGE normalized $MW_{app}$ of the 3.5 $\mu$g bands. A strong correlation exists between the two variables ($r = 0.88$; $r^2 = 0.77$), indicating that the shift in $MW_{app}$ of the bands in SDS-PAGE is associated with an increase in the fraction of dimer. The peptides in the graph appear to separate into two broad groups, where the more polar amino acids (Glu, Gln, Gly, Asn, Thr, Ser, His, and Ala) are clustered on the lower left quadrant and the less polar residues (Phe, Leu, Val, and Ile) are at the upper right quadrant. The dependence of oligomeric state on peptide concentration may also explain the differences seen for TM2-H and TM2-A on SDS-PAGE (ability to dimerize at high concentrations) versus SDS-FRET (decreased ability to dimerize). The peptide concentration used in the latter may not be high enough to allow these peptides to dimerize. This suggests that His and Ala mutations result in less stable dimers relative to those from Phe, Leu, Val, and Ile mutations (which can dimerize under both experimental conditions) and more stable dimers compared to the remaining mutants (which show decreased ability to dimerize under both experimental conditions).

Competition FRET experiments showed that the quenching of the donor peptide fluorescence by the acceptor peptide is due to a specific interaction of the helices rather than just non-specific colocalization because the fluorescence can be rescued by the addition of unlabeled peptide (see Supporting Information Figure S2).

**C-terminal Amino Acid Identity Affects TM Segment Helicity.** To determine the effect of the Phe-90 mutations on the secondary structure of the peptide, we utilized CD spectroscopy. The Phe-90 mutated peptides displayed $\alpha$-helical secondary structure in SDS micelles (Figure 3A). Figure 3B quantifies the percent helicity for each peptide compared to the TM2-F wild type. In general, the more polar amino acids (Glu, Gly, Gln, Asn, Ser, Thr, Ala, and His) showed a significant decrease in $\alpha$-helicity, whereas the less polar amino acids either increased $\alpha$-helicity or had no statistically significant effect relative to that of TM2-F.

To ensure that the observed change in $\alpha$-helicity is not due to a change in helix propensity caused by amino acid mutations, the percent helicity for each peptide was plotted against helix

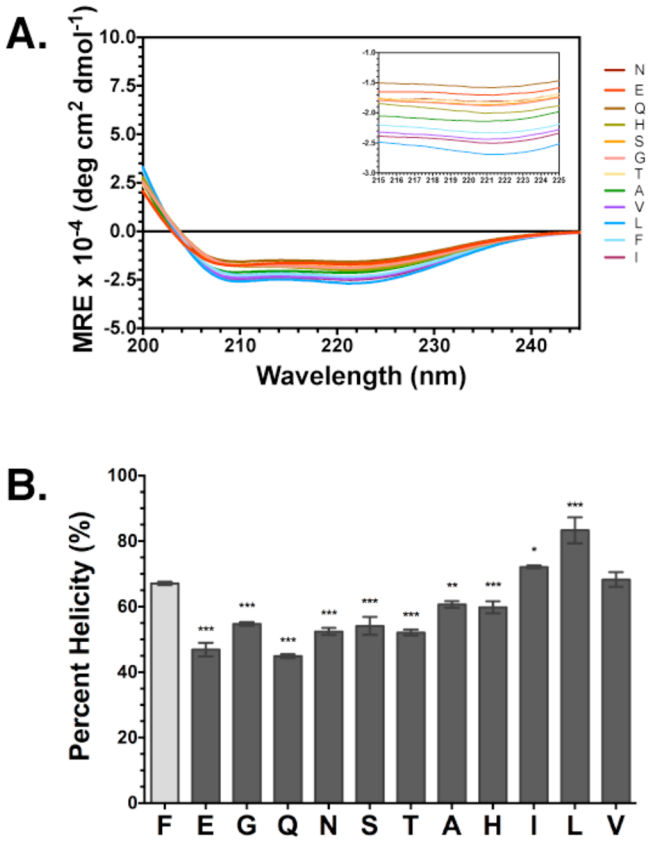


**Figure 3.** CD analysis of the Phe-90 mutated TM2-F peptides. (A) CD spectra of the TM2-F Phe-90 mutated peptides (15 $\mu$M) in 105 mM SDS, 10 mM borate, 10 mM phosphate, and 10 mM acetate (pH 7.3). The inset figure shows an expanded view of the spectra near 222 nm. (B) Percent helicity of the TM2-F Phe-90 mutated peptides. Error bars correspond to the standard deviation of at least three experiments. $p$ values were generated from multiple comparison tests (with the Dunnett correction applied). *, $p < 0.05$; **, $p < 0.01$; ***, $p < 0.001$.

propensity values derived from experimental studies of proteins and peptides.[29] The results indicate that there is no statistically significant correlation between percent helicity and helix propensity for the TM2 peptides (data not shown). This is in agreement with previous studies showing that peptide helicity in SDS micelles is largely governed by hydrophobicity rather than helix propensity.[30]

In order to determine the relationship between TM helix–helix interactions and peptide secondary structure, the results from the SDS-PAGE and SDS-FRET experiments were plotted against the percent helicity obtained from CD (Figure 4). Plots for both SDS-PAGE and SDS-FRET show strong statistically significant correlations between peptide interactions and secondary structure ($r = 0.97$ and −0.78, respectively; $p < 0.01$). As the percent helicity of the peptide decreases, there is a corresponding decrease in helix–helix interactions (and *vice versa*).

**Determining the Residues Mediating TM2 Helix–Helix Interactions.** Additional amino acid mutations were introduced to the C-terminus of the TM2-F peptide near the Phe-90 position in order to elucidate the key residues mediating its ability to self-associate (Table 2). TM amino acids with small side chain volumes (Ala-83, Ala-87, and Gly-89) were mutated individually to a larger amino acid (Val) in order to disrupt any potential van der Waals packing interactions. These


dx.doi.org/10.1021/bi500317h | *Biochemistry* 2014, 53, 3747–3757

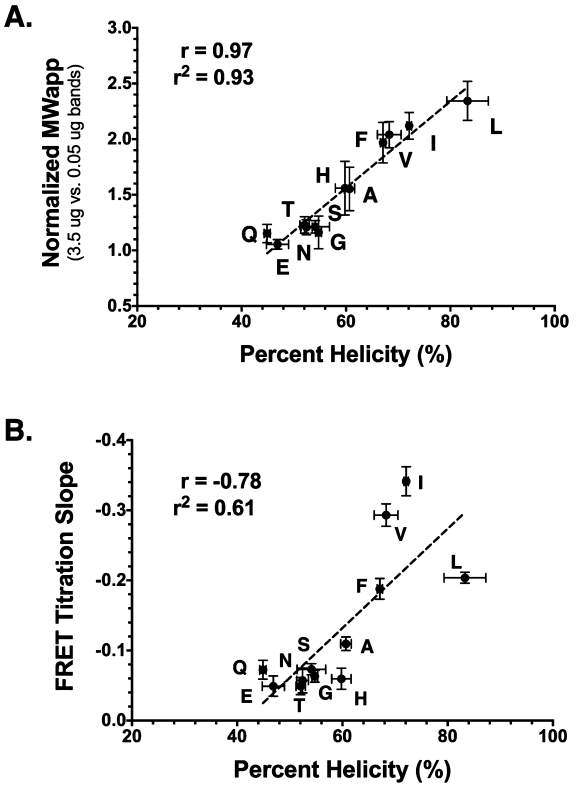


**Figure 4.** Correlation analysis of helix–helix interactions and peptide $\alpha$-helicity. (A) Normalized $MW_{app}$'s of the 3.5 $\mu$g bands from SDS-PAGE and (B) slopes determined from the SDS-FRET titration experiments were plotted against the percent helicity determined from the CD experiments. The dotted line represents the best linear fit. Error bars correspond to the standard deviation of the mean.

interactions are known to be involved in the association and assembly of TM $\alpha$-helices in many other membrane proteins.[31] Similarly, TM amino acids with large side chain volumes (Tyr-81, Leu-84, and Leu-86) were mutated individually to a smaller amino acid (Ala). Glu88 was mutated to a glutamic acid 5-methyl-ester ($Glu^{me}$) to determine whether this residue contributes to peptide self-association through H-bonding and/or ion-pairing.

Figures 5 and S4 show the effects of these mutations on their migration profiles in SDS-PAGE as a function of peptide loading amount. The majority of the mutant peptides exhibited concentration-dependent migration behavior similar to that of wild-type TM2-F. The L86A peptide also showed a change in migration as a function of peptide concentration, but this effect was dampened compared to that of the wild-type peptide.

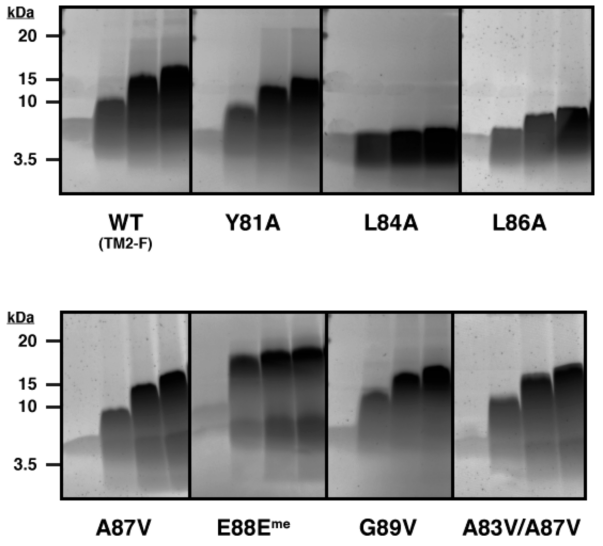


**Figure 5.** SDS-PAGE analysis of the TM2-F mutations near the helix terminus. TM2-F and the mutant peptides were loaded onto 18% Tris-glycine gels at increasing amounts of peptide: 0.05, 1.0, 2.5, and 3.5 $\mu$g (increasing from left to right per gel). The gels were stained and visualized using Sypro Ruby protein stain.

L84A, on the other hand, lacked any titration-dependent behavior.

Figure 6 shows the results from the SDS-FRET titration experiments. The linear titration profiles of these peptides indicate dimeric interactions with the variation in slopes, suggesting differences in the fraction of dimers. A87V, G89V, A83V/A87V, and $E88E^{me}$ resulted in a greater slope than that of WT TM2-F, whereas L84A showed a statistically significant decrease ($p < 0.001$). Both the Y81A and L86A mutations had no statistically significant effects on the TM2-F helix–helix interactions.

Figure 7 shows the CD analysis of the peptides. All of the mutants were $\alpha$-helical. A87V ($p < 0.05$), A83V/A87V ($p < 0.05$), and $E88E^{me}$ ($p < 0.001$) had a higher percent helicity compared to that of the WT peptide, whereas both L84A and L86A ($p < 0.001$) had reduced helicities. Y81A and G89V showed no statistically significant effects.

**Local Hydrophobicity of the Helix C-terminus Modulates Helix–Helix Interactions and Helicity.** To test whether the changes in helix–helix interactions and $\alpha$-helicity caused by the amino acid mutations were due to a change in hydrophobicity of the peptide terminus, we plotted the SDS-FRET titration slopes and percent helicity versus the hydrophobicity of the amino acid mutations (based on the $\Delta G_{app}$'s from the biological hydrophobicity scale[32]). The

**Table 2. Sequences of the PLP TM2-F Peptides Containing Helix–Helix Interaction Mutations**

| peptide | sequence[a] | MW (Da) |
|---|---|---|
| WT (TM2-F) | KKKK-AFQYVIYGTASFFFLYGALLLAEGF-KKKK | 3834 |
| Y81A | KKKK-AFQYVIYGTASFFFL**A**GALLLAEGF-KKKK | 3743 |
| L84A | KKKK-AFQYVIYGTASFFFLYGA**A**LLAEGF-KKKK | 3793 |
| L86A | KKKK-AFQYVIYGTASFFFLYGALL**A**AEGF-KKKK | 3793 |
| A87V | KKKK-AFQYVIYGTASFFFLYGALLL**V**EGF-KKKK | 3863 |
| $E88E^{me}$ | KKKK-AFQYVIYGTASFFFLYGALLLA**E$^{me}$**GF-KKKK | 3848 |
| G89V | KKKK-AFQYVIYGTASFFFLYGALLLAE**V**F-KKKK | 3877 |
| A83V/A87V | KKKK-AFQYVIYGTASFFFLYG**V**LLL**V**EGF-KKKK | 3891 |

[a]Mutated residues are underlined; $E^{me}$ = glutamic acid 5-methyl-ester


dx.doi.org/10.1021/bi500317h | *Biochemistry* 2014, 53, 3747–3757

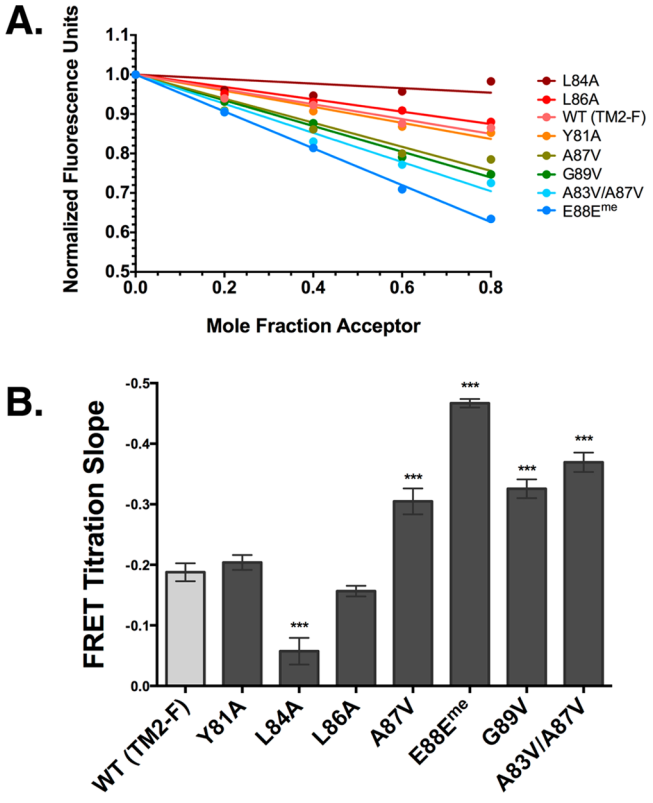


**Figure 6.** SDS-FRET dabsyl titration analysis of the TM2-F peptides containing putative helix–helix interaction mutations. (A) SDS-FRET titration. Dansyl-labeled peptides (donor) were titrated with an increasing mole fraction of dabsyl-labeled peptides (acceptor) in 70 mM SDS, 10 mM borate, 10 mM phosphate, and 10 mM acetate (pH 7.3). The total peptide concentration was kept constant at 10 $\mu$M by the addition of unlabeled peptide. Dansyl-labeled donor peptides were excited at 341 nm, and emission was measured from 450 to 650 nm. Plots were generated and data were fit as described in the Experimental Procedures; the lines shown represent the best fit to each data set. Error bars correspond to the standard deviation of at least three experiments. (B) FRET slope analysis. The slopes from the linear fit of the FRET titration data were extracted and plotted. Error bars correspond to the standard error of the mean. The mutant peptides were compared to WT TM2-F using the Dunnet multiple comparison test. ***, $p < 0.001$.

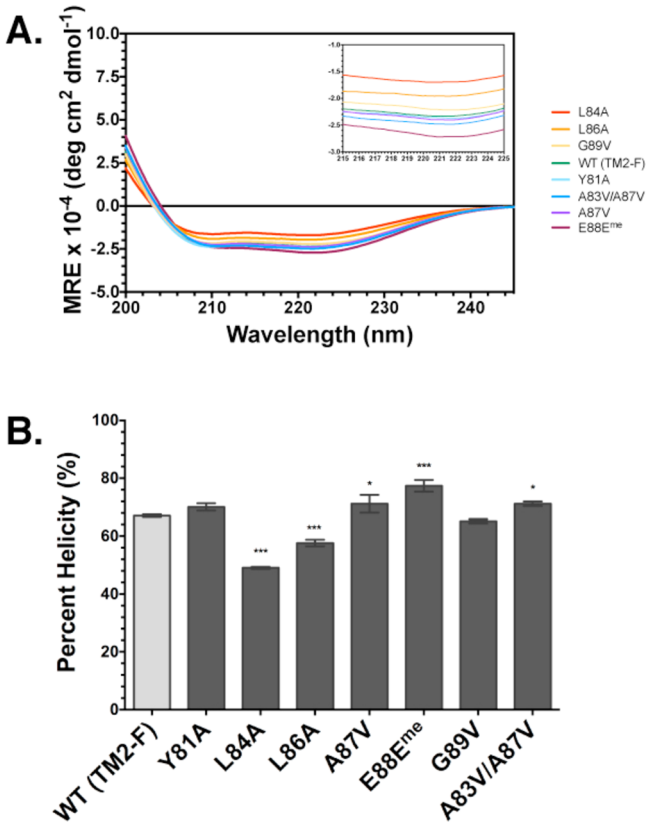


**Figure 7.** CD analysis of the TM2 peptides containing putative helix–helix interaction mutations. (A) CD spectra of TM2-F mutant peptides (15 $\mu$M) in 105 mM SDS, 10 mM borate, 10 mM phosphate, and 10 mM acetate (pH 7.3). The inset figure shows an expanded view of the spectra near 222 nm. (B) Percent helicity of TM2-F mutant peptides. Error bars correspond to the standard deviation of at least three experiments. $p$ values were generated from multiple comparison tests (with the Dunnett correction applied). *, $p < 0.05$; **, $p < 0.01$; ***, $p < 0.001$.

TM2F-E88E$^{me}$ peptide could not be plotted on the graph because of its unknown hydrophobicity on this scale. Figure 8 shows that there is an effect on the helix–helix interactions and helicity of the peptides mediated by amino acid hydrophobicity. As the hydrophobicity is increased, there is an increase in both helix–helix interactions and helicity. We hypothesized that this effect is due to the folding of the peptide occurring in two sequential stages: (i) TM partitioning of the C-terminus into the detergent, which increases $\alpha$-helicity (eq 1A) and (ii) the interaction of the peptide monomers to form dimers (eq 1B). The following model describes this process and was used to fit the data (see Supporting Information S5 for the derivations of the equations used for fitting)

$$P_{H_2O,mon} \overset{K_{app}}{\longleftrightarrow} P_{SDS,mon} \quad (1A)$$

$$2P_{SDS,mon} \overset{K_d}{\leftrightarrow} P_{SDS,dim} \quad (1B)$$

where $P_{H_2O,mon}$ is the concentration of monomeric peptide with its C-terminus partially exposed to aqueous buffer, $P_{SDS,mon}$ is the concentration of monomeric peptide (with its C-terminus solvated by detergent) in SDS, and $P_{SDS,dim}$ is the concentration of dimeric peptide (with its C-terminus solvated by detergent) in SDS. $K_{app}$ and $K_d$ are the equilibrium constants for the partitioning of the C-terminus from the aqueous to the detergent phase and the dissociation of the peptide dimer into monomers, respectively.

This model fits well with both the FRET and CD data (adjusted $r^2$ values of 0.94 and 0.89, respectively). Similar results were obtained when fitting the data using other hydrophobicity scales such as the octanol and octanol-interface scales (data not shown).[33,34] This indicates that our assumption that the $K_d$ remains the same among the peptides is reasonable. Alternatively, the partitioning of the TM peptide into the detergent may dominate the overall reaction. The best-fit values for the $K_d$ showed good agreement between both data sets ($K_{d,FRET}$ = 0.030 ± 0.003 mM and $K_{d,CD}$ = 0.037 ± 0.1 mM). The fit of the CD data resulted in a percent helicity for the peptide of 49 ± 2% in the aqueous phase and 75 ± 3% in the SDS phase.


dx.doi.org/10.1021/bi500317h | *Biochemistry* 2014, 53, 3747–3757

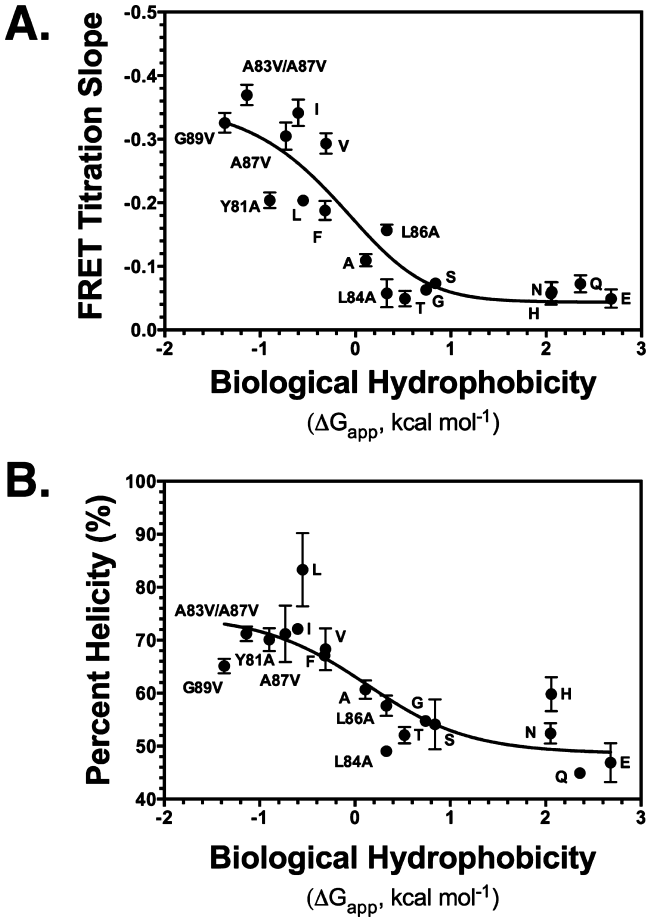


**Figure 8.** Role of local hydrophobicity on TM helix–helix interactions and $\alpha$-helicity. (A) Titration slopes from SDS-FRET and (B) percent helicity determined from CD experiments of each peptide were plotted against the $\Delta G_{app}$ derived from the biological hydrophobicity scale[32] (where increasing values of $\Delta G_{app}$ indicate decreasing peptide hydrophobicity). The curves represent the best nonlinear regression fit of the data based on hypothetical models describing the relationships among hydrophobicity, helicity, and helix–helix interactions (see Supporting Information Figure S4). Error bars correspond to the standard deviation of the means ($n$ = 3).

## DISCUSSION

The TM segments of PLP contain multiple potential helix–helix interaction sequence motifs that may play a role in the ability of the protein to oligomerize.[35] In addition, the sensitivity of this protein's oligomeric state to membrane compartments (i.e., ER vs plasma membrane) as well as to disease-causing point mutations suggests that factors such as helix–lipid interactions may be modulating the extent of helix–helix interactions.[11,12] As such, studying these TM segments may reveal additional factors, besides sequence motifs, that can modulate TM helix–helix interactions in general.

In a previous study, we showed that the $\alpha$-helicity and self-association of the PLP TM2 segment are extremely sensitive to the presence or absence of Phe-90 at its C-terminus, suggesting that this region may play a role in modulating the peptide's properties.[16] To systematically investigate this phenomenon, we prepared two libraries of PLP TM2-F mutants. In one set of peptides, wild-type Phe-90 was mutated to a wide range of amino acids in order to evaluate the sensitivity of helix–helix association to the side chain character of the peptide C-terminus. Our data suggest that the local hydrophobicity affects the degree of peptide partitioning from the aqueous to the detergent phase followed by the interaction of the helices to form dimers (eqs 1A and 1B and Figure 9). This process is highly coupled, and a slight change in hydrophobicity can severely affect the stability of the resulting dimers. The peptide is perhaps most sensitive to hydrophobicity changes when its local C-terminal hydrophobicity is somewhere near the hydrophobicity of Ala ($\Delta G_{app} \approx 0$ kcal mol$^{-1}$ on the biological hydrophobicity scale determined via the inflection points of the fitted curves in Figure 8). In addition, there appears to be a minimum threshold hydrophobicity ($\Delta G_{app} \approx 1.6$ kcal mol$^{-1}$) that must be satisfied before the TM segment can increase in $\alpha$-helicity and dimerize. Intriguingly, the TM2-H peptide shows significant tendency to dimerize (Figure 1) and maintains helicity similar to TM2-A, a result that we attribute to the deprotonated (neutral) state of the imidazole ring at the high pH imposed by the SDS-PAGE experiment (operating pH of ca. 9.5).[36] The presence of cation–$\pi$ interactions between the imidazole ring and neighboring Lys residues should also be considered.[37]

We further observed that partitioning of the TM2-F peptide from the aqueous to the detergent phase likely involves only a portion of the TM segment. The percent helicity of the monomer species in the aqueous phase is ca. 50%, which, for a 33-residue peptide, equates to 17 residues that have an $\alpha$-helical secondary structure. In contrast, in a sample lacking any detergent, the peptide has minimal, if any, $\alpha$-helicity.[16] This suggests that in the presence of SDS, peptides in the aqueous phase are partially bound to SDS molecules (which are known to induce $\alpha$-helicity[26]). Increasing the hydrophobicity of the peptide likely allows SDS to bind to regions that were previously uncoated, further increasing peptide helicity. In the case of our peptides, the region that partitions between the aqueous and SDS phase is likely localized to the C-terminus, as our mutations targeted residues only in this area.

We determined an apparent $K_d$ for the TM2-F peptide interaction of approximately 0.030 mM. The interpretation of this value and the comparison to dissociation constants derived from other TM segments are complicated by the detergent environment. For example, the apparent $K_d$ for the dimerization of GpA in SDS varied between 0.6–10 $\mu$M as the detergent concentration was increased from 1.2–25 mM.[38] In general, as SDS concentration increases, the interaction affinity of TM segments decrease (i.e., $K_d$ increases). Our experiments utilized SDS concentrations ranging from 70–105 mM. This high amount of SDS versus the much lower concentration of peptide in our samples (10–15 $\mu$M) could explain why the value of the FRET titration slopes (which approximate the fraction of dimers) reached a plateau of ca. −0.34 at high hydrophobicity rather than a value of −1.

In a second set of peptides, we varied the side chain type and volume of residues likely to participate in the helix–helix interface. Mutations targeting potential helix–helix association motifs (e.g., Ala-83, Ala-87, and Gly-89) and other nearby residues (Tyr-81, Leu-84, and Leu-86) did not reveal any obvious helix–helix interaction surface(s) near the C-terminus because of the extreme sensitivity of this TM peptide to changes in hydrophobicity. As the hydrophobicity of these mutations increased (or decreased), the helix–helix interactions and $\alpha$-helicity changed in a similar fashion. The E88E$^{me}$ mutation retained the ability to dimerize, which indicates that the dimer interaction is not mediated by H-bonding or ion-pair


dx.doi.org/10.1021/bi500317h | Biochemistry 2014, 53, 3747–3757

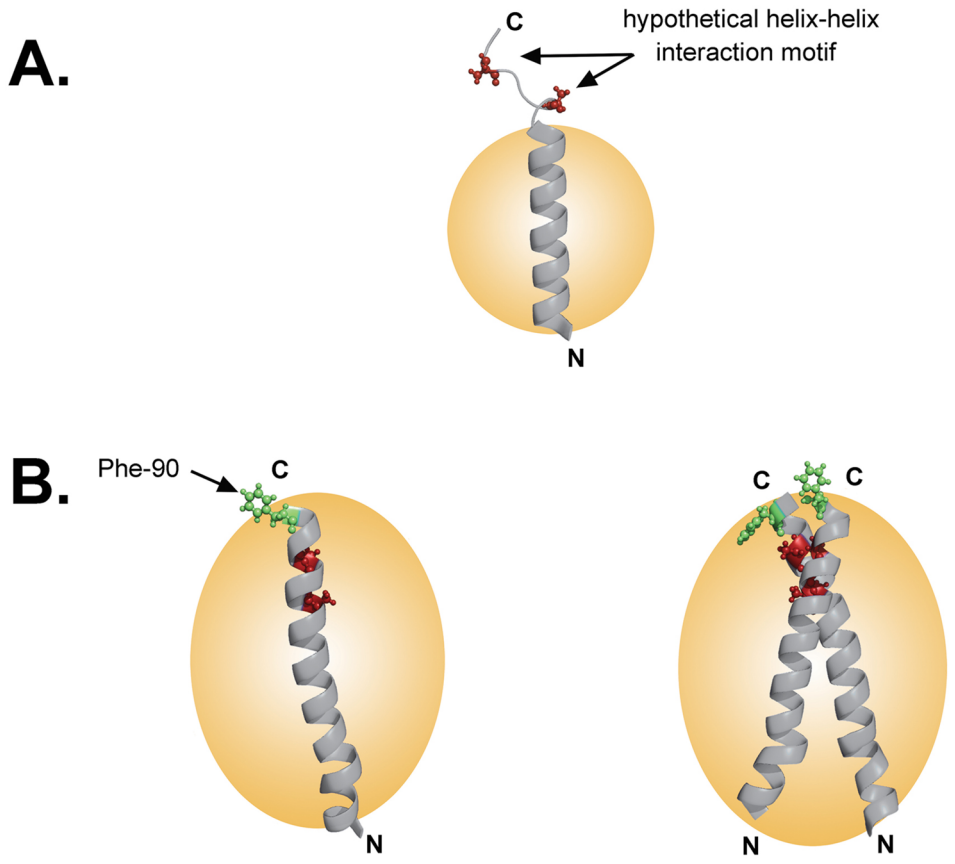


**Figure 9.** Hypothetical schematic modeling the effect of terminal hydrophobicity on the $\alpha$-helicity and self-association of PLP TM2. (A) A decrease in the hydrophobicity of the TM2 C-terminus destabilizes local peptide−detergent interactions. This results in a loss of $\alpha$-helicity at the C-terminus and a disruption of potential helix−helix interactions. (B) An increase in the hydrophobicity of the C-terminus stabilizes local peptide−detergent interactions. As a result, the C-terminus is $\alpha$-helical, and helix−helix interactions are maintained. In panel A vs B, the micelle size has been adjusted to reflect the degree of peptide insertion.

interactions involving Glu-88. Further high-resolution structural studies where the local hydrophobicity of the TM2 C-terminus is not modified (e.g., NMR) will be required to conclusively determine the actual role, if any, of these putative helix−helix association motifs in interhelix packing.

Our FRET data indicate that this peptide most likely interacts in a symmetric fashion, because this peptide undergoes a monomer−dimer equilibrium.[38] A peptide that interacts asymmetrically would proliferate and form greater-than-dimer species because there is a "sticky" surface that is not completely satisfied by a single pairwise configuration.[39] Although the present study did not identify a specific helix−helix interaction-compatible surface on this peptide, it is likely that one exists. As seen in another TM peptide that consisted solely of Leu, the highly hydrophobic nature of this peptide was not sufficient for dimerization in SDS and required the presence of an H-bonding-capable residue in order to form dimers.[40]

The functional relevance of PLP oligomerization is not known. However, disease-causing point mutations can result in premature oligomerization and retention in the ER, leading to Pelizaeus−Merzbacher disease and spastic paraplegia type 2;[11,12] indeed, more than 40% of these point mutations occur in the PLP TM.[35] With regard to the mutations that target the putative helix−helix interaction motifs, the results were inconclusive because of the highly sensitive nature of the TM peptide to hydrophobicity changes. Nevertheless, we note that the L86A (but not the L84A) mutation adds a new "small-XXX-small" motif (in this case, $^{82}$GALLA$^{86}$), which may explain why the helicity and apparent extent of dimerization are higher for the L86A mutant despite the identical hydrophobicity change as L84A.

## ■ CONCLUSIONS

Experiments with TM peptides where the C-terminal residue is systematically varied show that the alteration of local hydrophobicity can ultimately affect both helix−helix interactions and segment $\alpha$-helicity. These findings suggest that a given change to the local hydrophobicity and/or membrane interaction near the helix C-terminus (and possibly the N-terminus) can have a major effect on the properties of the corresponding TM $\alpha$-helix. Although our findings may be limited by the peptide-based approach of the current study, it is possible that this phenomenon may be a common mechanism for the regulation of membrane protein structure and activity. For example, post-translational modifications (such as phosphorylation, acylation, glycosylation, etc.) or disease-causing point mutations of these residues might lead to a change in local hydrophobicity that affects the secondary and tertiary/quaternary structure of the TM helices and hence the overall structure/activity of the protein.


dx.doi.org/10.1021/bi500317h | *Biochemistry* 2014, 53, 3747−3757

## ■ ASSOCIATED CONTENT

### Supporting Information

Effect of Phe-90 mutations on SDS-PAGE peptide migration; competition FRET experiment of PLP TM2-F; correlation analysis of SDS-PAGE $MW_{app}$ versus SDS-FRET titration slope; effect of TM2-F mutations near the helix terminus on SDS-PAGE migration; and derivation of equations describing the relationship among helix−helix interactions, helicity, and hydrophobicity for fitting FRET and CD data. This material is available free of charge via the Internet at http://pubs.acs.org.

## ■ AUTHOR INFORMATION


### Corresponding Author

*Tel.: (01) 416 813-5924; Fax: (01) 416 813-5005; E-mail: deber@sickkids.ca.



### Funding

Supported, in part, by a grant to C.M.D. from the Canadian Institutes of Health Research (CIHR FRN-5810). D.P.N. held a Frederick Banting and Charles Best Canada Graduate Scholarship (CGS) Doctoral Award from CIHR.


### Notes

The authors declare no competing financial interest.

## ■ ABBREVIATIONS USED

PLP, proteolipid protein; TM, transmembrane; SDS, sodium dodecyl sulfate; FRET, fluorescence resonance energy transfer; DMF, dimethylformamide; DIEA, *N*,*N*-diisopropylethylamine; HATU, *O*-(7-azabenzotriazol-1-yl)-*N*,*N*,*N*′,*N*′-tetramethyluronium hexafluorophosphate; PAL, peptide amide linker; PEG, poly(ethylene glycol); PS, polystyrene; TFA, trifluoroacetic acid; TIPS, triisopropylsilane; RP-HPLC, reverse-phase high-performance liquid chromatography; MW, molecular weight; CD, circular dichroism; TFE, 2,2,2-trifluoroethanol; $MW_{app}$, molecular weight apparent; GpA, glycophorin A; WT, wild type; $E^{me}$, glutamic acid 5-methyl ester

## ■ REFERENCES


(1) Popot, J. L., and Engelman, D. M. (1990) Membrane protein folding and oligomerization: the two-stage model. *Biochemistry 29*, 4031−4037.

(2) Li, E., Wimley, W. C., and Hristova, K. (2012) Transmembrane helix dimerization: beyond the search for sequence motifs. *Biochim. Biophys. Acta 1818*, 183−193.

(3) Wehbi, H., Rath, A., Glibowicka, M., and Deber, C. M. (2007) Role of the extracellular loop in the folding of a CFTR transmembrane helical hairpin. *Biochemistry 46*, 7099−7106.

(4) Anbazhagan, V., and Schneider, D. (2010) The membrane environment modulates self-association of the human GpA TM domain − implications for membrane protein folding and transmembrane signaling. *Biochim. Biophys. Acta 1798*, 1899−1907.

(5) Curran, A. R., Templer, R. H., and Booth, P. J. (1999) Modulation of folding and assembly of the membrane protein bacteriorhodopsin by intermolecular forces within the lipid bilayer. *Biochemistry 38*, 9328−9336.

(6) Khemtémourian, L., Buchoux, S., Aussenac, F., and Dufourc, E. J. (2007) Dimerization of Neu/Erb2 transmembrane domain is controlled by membrane curvature. *Eur. Biophys. J. 36*, 107−112.

(7) Hong, H., and Bowie, J. U. (2011) Dramatic destabilization of transmembrane helix interactions by features of natural membrane environments. *J. Am. Chem. Soc. 133*, 11389−11398.

(8) Thévenin, D., Roberts, M. F., Lazarova, T., and Robinson, C. R. (2005) Identifying interactions between transmembrane helices from the adenosine A2A receptor. *Biochemistry 44*, 16239−16245.

(9) Simons, K., and Toomre, D. (2000) Lipid rafts and signal transduction. *Nat. Rev. Mol. Cell Biol. 1*, 31−39.

(10) Simons, K., and Vaz, W. L. C. (2004) Model systems, lipid rafts, and cell membranes. *Annu. Rev. Biophys. Biomol. Struct. 33*, 269−295.

(11) Swanton, E., Holland, A., High, S., and Woodman, P. (2005) Disease-associated mutations cause premature oligomerization of myelin proteolipid protein in the endoplasmic reticulum. *Proc. Natl. Acad. Sci. U.S.A. 102*, 4342−4347.

(12) Dhaunchak, A. S., Colman, D. R., and Nave, K.-A. (2011) Misalignment of PLP/DM20 transmembrane domains determines protein misfolding in Pelizaeus−Merzbacher disease. *J. Neurosci. 31*, 14961−14971.

(13) Mitra, K., Ubarretxena-Belandia, I., Taguchi, T., Warren, G., and Engelman, D. M. (2004) Modulation of the bilayer thickness of exocytic pathway membranes by membrane proteins rather than cholesterol. *Proc. Natl. Acad. Sci. U.S.A. 101*, 4083−4088.

(14) Pelttari, A., and Helminen, H. J. (1979) The relative thickness of intracellular membranes in epithelial cells of the ventral lobe of the rat prostate. *Histochem. J. 11*, 613−624.

(15) Cuthbertson, J. M., Doyle, D. A., and Sansom, M. S. P. (2005) Transmembrane helix prediction: a comparative evaluation and analysis. *Protein Eng., Des. Sel. 18*, 295−308.

(16) Ng, D. P., and Deber, C. M. (2010) Deletion of a terminal residue disrupts oligomerization of a transmembrane alpha-helix. *Biochem. Cell Biol. 88*, 339−345.

(17) Merrifield, R. B. (1969) Solid-phase peptide synthesis. *Adv. Enzymol. Relat. Areas Mol. Biol. 32*, 221−296.

(18) Rath, A., Cunningham, F., and Deber, C. M. (2013) Acrylamide concentration determines the direction and magnitude of helical membrane protein gel shifts. *Proc. Natl. Acad. Sci. U.S.A. 110*, 15668−15673.

(19) Chen, Y. H., Yang, J. T., and Chau, K. H. (1974) Determination of the helix and beta form of proteins in aqueous solution by circular dichroism. *Biochemistry 13*, 3350−3359.

(20) Gans, P. J., Lyu, P. C., Manning, M. C., Woody, R. W., and Kallenbach, N. R. (1991) The helix-coil transition in heterogeneous peptides with specific side-chain interactions: theory and comparison with CD spectral data. *Biopolymers 31*, 1605−1614.

(21) Melnyk, R. A., Partridge, A. W., Yip, J., Wu, Y., Goto, N. K., and Deber, C. M. (2003) Polar residue tagging of transmembrane peptides. *Biopolymers 71*, 675−685.

(22) Adair, B. D., and Engelman, D. M. (1994) Glycophorin A helical transmembrane domains dimerize in phospholipid bilayers: a resonance energy transfer study. *Biochemistry 33*, 5539−5544.

(23) Li, M., Reddy, L. G., Bennett, R., Silva, N. D., Jones, L. R., and Thomas, D. D. (1999) A fluorescence energy transfer method for analyzing protein oligomeric structure: application to phospholamban. *Biophys. J. 76*, 2587−2599.

(24) Ulmschneider, M. B., and Sansom, M. S. (2001) Amino acid distributions in integral membrane protein structures. *Biochim. Biophys. Acta 1512*, 1−14.

(25) Killian, J. A., and von Heijne, G. (2000) How proteins adapt to a membrane−water interface. *Trends Biochem. Sci. 25*, 429−434.

(26) Rath, A., Glibowicka, M., Nadeau, V. G., Chen, G., and Deber, C. M. (2009) Detergent binding explains anomalous SDS-PAGE migration of membrane proteins. *Proc. Natl. Acad. Sci. U.S.A. 106*, 1760−1765.

(27) Anbazhagan, V., Cymer, F., and Schneider, D. (2010) Unfolding a transmembrane helix dimer: a FRET study in mixed micelles. *Arch. Biochem. Biophys. 495*, 159−164.

(28) Gimpelev, M., Forrest, L. R., Murray, D., and Honig, B. (2004) Helical packing patterns in membrane and soluble proteins. *Biophys. J. 87*, 4075−4086.

(29) Pace, C. N., and Scholtz, J. M. (1998) A helix propensity scale based on experimental studies of peptides and proteins. *Biophys. J. 75*, 422−427.

(30) Li, S. C., and Deber, C. M. (1993) Peptide environment specifies conformation. Helicity of hydrophobic segments compared in

aqueous, organic, and membrane environments. *J. Biol. Chem. 268*, 22975−22978.
(31) Ng, D. P., Poulsen, B. E., and Deber, C. M. (2012) Membrane protein misassembly in disease. *Biochim. Biophys. Acta 1818*, 1115−1122.
(32) Hessa, T., Kim, H., Bihlmaier, K., Lundin, C., Boekel, J., Andersson, H., Nilsson, I., White, S. H., and von Heijne, G. (2005) Recognition of transmembrane helices by the endoplasmic reticulum translocon. *Nature 433*, 377−381.
(33) White, S. H., and Wimley, W. C. (1999) Membrane protein folding and stability: physical principles. *Annu. Rev. Biophys. Biomol. Struct. 28*, 319−365.
(34) Wimley, W. C., Creamer, T. P., and White, S. H. (1996) Solvation energies of amino acid side chains and backbone in a family of host−guest pentapeptides. *Biochemistry 35*, 5109−5124.
(35) Ng, D. P., and Deber, C. M. (2010) Modulation of the oligomerization of myelin proteolipid protein by transmembrane helix interaction motifs. *Biochemistry 49*, 6896−6902.
(36) Hachmann, J. P., and Amshey, J. W. (2005) Models of protein modification in Tris-glycine and neutral pH Bis-Tris gels during electrophoresis: effect of gel pH. *Anal. Biochem. 342*, 237−245.
(37) Johnson, R. M., Hecht, K., and Deber, C. M. (2007) Aromatic and cation-pi interactions enhance helix−helix association in a membrane environment. *Biochemistry 46*, 9208−9214.
(38) Fisher, L. E., Engelman, D. M., and Sturgis, J. N. (1999) Detergents modulate dimerization, but not helicity, of the glycophorin A transmembrane domain. *J. Mol. Biol. 293*, 639−651.
(39) Rath, A., and Deber, C. M. (2007) Membrane protein assembly patterns reflect selection for non-proliferative structures. *FEBS Lett. 581*, 1335−1341.
(40) Zhou, F. X., Merianos, H. J., Brünger, A. T., and Engelman, D. M. (2001) Polar residues drive association of polyleucine transmembrane helices. *Proc. Natl. Acad. Sci. U.S.A. 98*, 2250−2255.